Photoluminescence dynamics of cavity polaritons under resonant excitation in the picosecond range

J. Bloch* and J. Y. Marzin
Laboratoire de Microstructures et de Microélectronique, CNRS, Boîte Postale 107, 92225 Bagneux Cedex, France
(Received 27 January 1997)

We present a calculation of time-resolved photoluminescence of cavity polaritons including scattering by acoustic phonons. Under resonant excitation to the lower-energy polariton, the calculated initial decay time, as a function of the detuning between the exciton and the cavity mode, is found to be in excellent agreement with the experimental measurements of Sermage *et al.* [Phys. Rev. B. 53, 16 516 (1996)]. Moreover, this model of perfectly delocalized polaritons describes qualitatively the overall dynamics under resonant excitation of the polariton states. However, the role of inhomogeneous broadening seems to be important to describe quantitatively the photoluminescence decay at long time delays. [S0163-1829(97)01627-5]

I. INTRODUCTION

Recently semiconductor microcavities have been fabricated and showed characteristic features of the strong coupling between the exciton and the cavity mode: the Rabi splitting has been measured in reflectivity, absorption as well as in photoluminescence.[1–5] The eigenstates of the system are exciton-photon mixed states, characterized by an in-plane wave vector, and named cavity polaritons. Their in-plane dispersion relation has been measured by angle-resolved photoluminescence.[2] Cavity effects are expected to modify the dynamics of spontaneous emission and several time-resolved luminescence experiments were performed in thin semiconductor microcavities to study spontaneous emission modification induced by cavity effect.[6–11] Recently, Sermage *et al.* reported picosecond photoluminescence measurements in a $\lambda/2$ semiconductor microcavity containing two quantum wells.[6] These experiments were performed for various detunings between the cavity mode and the exciton. When the lower-energy polariton was excited resonantly, a biexponential decay curve was measured. We interpreted this behavior in a similar way to Deveaud *et al.*:[12] the short time τ reflects the rapid initial decay of observed radiant states; the longer time reflects the refilling of these radiant states mainly from the reservoir of nonradiant excitons. In the cavity sample, the short decay τ appeared to be continuously reduced when the lower-energy state evolved, through a variation of the detuning, from an excitonlike state to a photonlike state. Simultaneously, the intensity of the signal corresponding to the second decay decreased continuously. In a rough approximation, we first described the evolution of the initial decay rate $1/\tau$, by a linear combination of a photon and an exciton decay rate ($1/\tau_c$ and $1/\tau_x$) weighted by the exciton and the photon component of the mixed state (x and c),

$$\frac{1}{\tau} = x\,\frac{1}{\tau_x} + c\,\frac{1}{\tau_c}. \tag{1}$$

The average exciton decay time τ_x should reflect overall inelastic scattering undergone by the exciton part of the polariton. This corresponds mainly to scattering by acoustic phonons.

We also presented time-resolved measurements of the low-energy polariton emission under excitation resonant to the high-energy polariton.[11] Under such a nonresonant excitation of the low-energy polariton, we also measured a clear dependence of the luminescence dynamics as a function of the detuning between the exciton and the cavity mode. Both the rise time and the decay time were continuously reduced when the lower-energy state evolved from an excitonlike to a photonlike state.

In this paper, we clarify the role of phonon scattering in these resonant photoluminescence experiments: we calculate the time evolution of the polariton population as a function of their in-plane wave vector using rate equations and including scattering by acoustic phonons. We deduce the time-dependent intensity of light emitted by the structure. Notice that acoustic-phonon scattering has already been included in the calculation of stimulated emission in a microcavity by Pau *et al.*[13] Moreover we compare our results with a recent paper of Tassone *et al.*,[14] where the temporal response of an analogous system under nonresonant excitation is considered.

The paper is organized as follows. First, we present the main ingredients of our polariton model. Then, we present calculated decay curves of the lower branch in two excitation configurations: (i) under resonant excitation of the lower polariton and (ii) under resonant excitation of the upper polariton. We finally compare our calculations with experimental measurements.

II. DESCRIPTION OF OUR MODEL

We describe the polariton states in a two-coupled band model, considering only the $1S$, $J=1$ state of the heavy-hole quantum well exciton with an in-plane dispersion relation given by

$$E_x(\mathbf{k}) = E_x^0 + \frac{\hbar^2|\mathbf{k}|^2}{2M}. \tag{2}$$

E_x^0 is the fundamental exciton energy and M is the effective mass describing the in-plane motion of the exciton center of mass. $M=m_e+m_h$, where m_e (m_h) is the electron (hole) in-plane mass.

The empty cavity mode has a dispersion given by

$$E_c(\mathbf{k})=\frac{\hbar v}{n_{\text{eff}}}\sqrt{k_0^2+|\mathbf{k}|^2}, \tag{3}$$

where n_{eff} is the cavity effective refraction index, v the speed of light, and k_0 and $\mathbf{k}$ the wave vectors along z and in the layer plane.

Since a planar microcavity has an in-plane translation invariance, each exciton with an in-plane wave vector $\mathbf{k}$ is coupled to the photon with the same in-plane wave vector. Therefore, the upper and lower branch polaritons with the in-plane wave vector $\mathbf{k}$ are approximated as the eigenstates of the 2×2 Hamiltonian:

$$H(\mathbf{k})=\begin{pmatrix} E_c(\mathbf{k}) & g \\ g^* & E_x(\mathbf{k}) \end{pmatrix}, \tag{4}$$

g is the radiative coupling between exciton and cavity modes. If u and l superscripts hold for the upper and lower polariton branches, these eigenstates are

$$|u(l)_k\rangle=x_{\mathbf{k}}^{u(l)}|X_{\mathbf{k}}\rangle+c_{\mathbf{k}}^{u(l)}|C_{\mathbf{k}}\rangle, \tag{5}$$

with

$$x_{\mathbf{k}}^u=\frac{g}{\sqrt{2\Delta(\delta+\Delta)}},$$

$$c_{\mathbf{k}}^u=\sqrt{(\delta+\Delta)/2\Delta},$$

$$x_{\mathbf{k}}^l=c_{\mathbf{k}}^u, \quad c_{\mathbf{k}}^l=-x_{\mathbf{k}}^u, \tag{6}$$

where $|C_{\mathbf{k}}\rangle$ and $|X_{\mathbf{k}}\rangle$ are the photon and exciton eigenstates at wave vector $\mathbf{k}$, respectively, and where

$$\delta=\frac{E_c(\mathbf{k})-E_x(\mathbf{k})}{2}, \quad \Delta=\sqrt{\delta^2+g^2}.$$

The eigenenergies are given by

$$E_{\mathbf{k}}^{u(l)}=\frac{E_c(\mathbf{k})+E_x(\mathbf{k})}{2}+(-)\,\frac{\Delta}{2}. \tag{7}$$

Acoustic phonons of wave vector $\mathbf{Q}=(\mathbf{q},q_z)$ can scatter a polariton from state $|i_{\mathbf{k}}\rangle$ to state $|f_{\mathbf{k}'}\rangle$ through the deformation potential Hamiltonian $H_{\text{def}}^{\mathbf{Q}}$ (taken from Ref. 15) coupling the corresponding excitons $|X_{\mathbf{k}}\rangle$ and $|X_{\mathbf{k}'}\rangle$. The transition rates between the two polariton states, of energy $E_{\mathbf{k}}$ and $E_{\mathbf{k}'}$, are given by

$$W_{\mathbf{k},\mathbf{k}'}=\frac{2\pi}{\hbar}\sum_{\mathbf{Q},\epsilon=\pm 1}|\langle i_{\mathbf{k}}|H_{\text{def}}^{\mathbf{Q}}|f_{\mathbf{k}'}\rangle|^2 \times\delta(E_{\mathbf{k}'}-E_{\mathbf{k}}-\epsilon\hbar\omega_{\mathbf{Q}})f_{\epsilon}(\hbar\omega_{\mathbf{Q}}), \tag{8}$$

where the phonon energy is $\hbar\omega_{\mathbf{Q}}$ and $f_{\epsilon}(\hbar\omega_{\mathbf{Q}})=n(\hbar\omega_{\mathbf{Q}})+(1-\epsilon)/2$ takes into account the phonon occupation number $n(\hbar\omega_{\mathbf{Q}})$ at a given temperature T. $\epsilon=1$ (-1) corresponds to the absorption (emission) of a phonon.

As in Ref. 14, we assume that the deformation potential matrix element between polariton states is simply given by the matrix element between exciton states multiplied by the respective exciton content of the polariton states, namely,

$$\langle i_{\mathbf{k}}|H_{\text{def}}^{\mathbf{Q}}|f_{\mathbf{k}'}\rangle=x_{\mathbf{k}}x_{\mathbf{k}'}\langle X_{\mathbf{k}}|H_{\text{def}}^{\mathbf{Q}}|X_{\mathbf{k}'}\rangle. \tag{9}$$

We assume that elastic scattering processes (due to alloy disorder and interface roughness) lead to a quick isotropic redistribution of polaritons in k space. Therefore, we calculate the population of rings in k space. Let N_k be the population of such a ring with radius k and thickness δk,

$$N_k=\rho_{2\text{D}}\,k\,dk\int_0^{2\pi}n(k,\theta)d\theta, \tag{10}$$

$n(k,\theta)$ is the occupation factor of the polariton state (k,θ) and $\rho_{2\text{D}}=S/4\pi^2$ the density of states in the two-dimensional phase space. The spin variable has been omitted here, because we do not consider spin-flipping scattering processes.

The rate equations for the time evolution of N_k, dropping the index of the branch from now on, are

$$\frac{dN_k}{dt}=-N_k\left(\frac{1}{\tau_k}+\sum_{k'}R_{k,k'}\right)+\sum_{k'}R_{k',k}N_{k'}+L_k(t), \tag{11}$$

with

$$R_{k,k'}=\rho_{2\text{D}}k'dk'\int_0^{2\pi}W_{\mathbf{k},\mathbf{k}'}d\theta. \tag{12}$$

In Eq. (12), θ is the angle between the initial and the final polariton wave vector $\mathbf{k}$ and $\mathbf{k}'$. $R_{k,k'}$ is the integrated scattering rate from the ring with radius k to the ring with radius k'. In Eq. (11), $1/\tau_k$ is the polariton escape rate which will be discussed later on, and $L_k(t)$ is the generation term.

The next step is to evaluate the averaged rates $R_{k,k'}$. For the sake of simplicity, the $1S$ exciton wave function is taken as the simplest variational trial function as in Ref. 13

$$\langle\mathbf{r}_e,\mathbf{r}_h|X_{\mathbf{k}}\rangle=\chi_e(z_e)\chi_h(z_h)F(\rho)\,\frac{1}{\sqrt{S}}\,e^{i\mathbf{K}\cdot\mathbf{R}}, \tag{13}$$

$\mathbf{r}_e$ and $\mathbf{r}_h$ are the in-plane coordinate vectors of the electron and hole, respectively, $\rho=|\mathbf{r}_e-\mathbf{r}_h|$, $\mathbf{R}$ is the in-plane position of the exciton center-of-mass, and $\mathbf{K}$ the associated wave vector. $\chi_e(z_e)$ and $\chi_h(z_h)$ are sine functions describing the wave functions for the electron or hole in a 12-nm quantum well for the case of infinite barriers. $F(r)$ is an exponential function describing the spatial extension of the exciton envelope function over the bore radius $\lambda=13$ nm.

Following Ref. 15, we take

$$H_{\text{def}}^{\mathbf{Q}}=\sqrt{\hbar Q/2\varphi Vu}(D_e e^{i\mathbf{Q}\mathbf{r}_e}+D_h(q,q_z)e^{i\mathbf{Q}\mathbf{r}_h}), \tag{14}$$

with

$$D_h(q,q_z)=\frac{l+m}{2}\,\frac{q^2}{Q^2}+m\,\frac{q_z^2}{Q^2}. \tag{15}$$

φ is the mass density, u the longitudinal sound velocity, V the sample volume, l and m the deformation potentials (taken from Ref. 15 for GaAs/Ga_xAl_{1-x}As quantum wells).

$Q=\sqrt{q^2+q_z^2}$ is the modulus of the (3D) phonon wave vector $\mathbf{Q}=(\mathbf{q},q_z)$. The deformation potential matrix elements are then given by

$$\langle X_{\mathbf{k}}|H_{\mathrm{def}}^{\mathbf{Q}}|X_{\mathbf{k}'}\rangle=\sqrt{\hbar Q/2\varphi Vu}D(q,q_z)A(q_z)\,\delta_{\mathbf{q},\mathbf{k}-\mathbf{k}'} \quad (16)$$

with

$$D(q,q_z)=D_eG\left(\frac{qm_h}{M}\right)+D_h(q,q_z)G\left(\frac{qm_e}{M}\right) \quad (17)$$

and where $A(q_z)$ and $G(x)$ are the Fourier transform of $\chi_e^2(z)$ and $F^2(\rho)$, respectively. Using Eqs. (9) and (16) in Eq. (8), we deduce

$$\begin{aligned}W_{\mathbf{k},\mathbf{k}'}=&\frac{\pi x_{\mathbf{k}}^2x_{\mathbf{k}'}^2}{\varphi Vu}\sum_{\mathbf{q}_z,\epsilon=\pm1}\sqrt{q_z^2+|\mathbf{k}-\mathbf{k}'|^2}\\&\times D^2(|\mathbf{k}'-\mathbf{k}|,q_z)A^2(q_z)\\&\times\delta(E_{\mathbf{k}'}-E_{\mathbf{k}}-\epsilon\hbar\omega_{|\mathbf{k}-\mathbf{k}'|,q_z})f_\epsilon(|E_{\mathbf{k}'}-E_{\mathbf{k}}|).\end{aligned} \quad (18)$$

The delta function in Eq. (18) selects a q_z value for the emitted or the absorbed phonon. Only for a sufficiently large difference in energy between the initial and the final state, both in-plane momentum and energy conservations are simultaneously possible. In this case, q_z is given by

$$q_z=\pm\sqrt{(K_{\mathbf{k},\mathbf{k}'})^2-|\mathbf{k}-\mathbf{k}'|^2}$$

with

$$K_{\mathbf{k},\mathbf{k}'}=\left|\frac{E_{\mathbf{k}'}-E_{\mathbf{k}}}{\hbar u}\right|. \quad (19)$$

$K_{\mathbf{k},\mathbf{k}'}$ is the modulus of the phonon wave vector. Equation (18) can be simply replaced by

$$\begin{aligned}W_{\mathbf{k},\mathbf{k}'}=&\frac{L_zx_{\mathbf{k}}^2x_{\mathbf{k}'}^2K_{\mathbf{k},\mathbf{k}'}}{\hbar\varphi Vu^2q_z}D^2(|\mathbf{k}'-\mathbf{k}|,q_z)A^2(q_z)\\&\times\delta(q_z-\sqrt{(K_{\mathbf{k},\mathbf{k}'})^2-|\mathbf{k}-\mathbf{k}'|^2})\\&\times f_{\mathrm{sgn}(E_{\mathbf{k}'}-E_{\mathbf{k}})}(|E_{\mathbf{k}'}-E_{\mathbf{k}}|)Y(K_{\mathbf{k},\mathbf{k}'}-|\mathbf{k}-\mathbf{k}'|)\end{aligned} \quad (20)$$

where a factor of 2 corresponding to $\pm q_z$ has been taken into account and where $Y(x)$ is the Heaviside function.

$R_{k,k'}$ thus reads from Eq. (12)

$$\begin{aligned}R_{k,k'}=&\frac{L_z\rho_{2\mathrm{D}}x_{\mathbf{k}}^2x_{\mathbf{k}'}^2k'dk'(K_{\mathbf{k},\mathbf{k}'})^2}{\hbar\varphi Vu^2}\\&\times\int_0^{2\pi}d\theta\,\frac{Y(K_{\mathbf{k},\mathbf{k}'}-|\mathbf{k}-\mathbf{k}'|)}{\sqrt{(K_{\mathbf{k},\mathbf{k}'})^2-|\mathbf{k}-\mathbf{k}'|^2}}\\&\times D^2[|\mathbf{k}-\mathbf{k}'|,\sqrt{(K_{\mathbf{k},\mathbf{k}'})^2-|\mathbf{k}-\mathbf{k}'|^2}]\\&\times A^2[\sqrt{(K_{\mathbf{k},\mathbf{k}'})^2-|\mathbf{k}-\mathbf{k}'|^2}]f_{\mathrm{sgn}(E_{\mathbf{k}'}-E_{\mathbf{k}})}(|E_{\mathbf{k}'}-E_{\mathbf{k}}|).\end{aligned} \quad (21)$$

In the detailed calculation, we are led to define several remarkable wave vectors.

(i) $k_{\mathrm{exc}}=1.4\times10^{-4}$ Å^{-1} is the in-plane wave vector of the polaritons created at the initial time. It is directly related to the experimental incidence angle of the excitation laser. The term $L_k(t)$ in Eq. (11) creates $N_0=10^{10}$ polaritons with an in-plane wave vector k_{exc} around the initial time.

(ii) Since the Bragg mirrors have a finite stop band, there is a given photon in-plane wave vector k_{cav}, at a given energy, beyond which the reflectivity drops down. For $k>k_{\mathrm{cav}}$, excitons $|X_{\mathbf{k}}\rangle$ and photon modes $|C_{\mathbf{k}}\rangle$ are in weak-coupling regime, the exciton being coupled to a continuum of photon modes. Therefore, for $k>k_{\mathrm{cav}}$, the two branches are associated to pure photon and exciton modes.

(iii) We also define $k_{\mathrm{rad}}=(n_{\mathrm{eff}}E_x^0)/\hbar c$ as the maximum in-plane wave vector of radiant exciton states. $k>k_{\mathrm{rad}}$ corresponds to nonradiant exciton states so that $1/\tau_k=0$. For $k_{\mathrm{cav}}<k<k_{\mathrm{rad}}$, we are in the weak-coupling zone of k space. Therefore, τ_k is simply the radiative lifetime of the exciton of wave vector k. In a rough approximation, we have taken a k-independent τ_k, equal to the zone-center radiative lifetime calculated with our variational exciton wave function. In summary, for $k_{\mathrm{cav}}<k<k_{\mathrm{rad}}$, $1/\tau_k=1/\tau_x=0.1$ ps^{-1}. For $k<k_{\mathrm{cav}}$, $1/\tau_k$ is equal to the polariton escape time c_k^2/τ_c. τ_c is the photon lifetime inside the cavity; in our case $\tau_c=1$ ps.

(iv) k_{obs} is the maximum in-plane wave vector of the polariton states emitting light within the detection cone and the collected signal during time dt is $I(t)=dt\Sigma_{k<k_{\mathrm{obs}}}N_k/\tau_k$. k_{obs} is slightly larger than k_{exc} to reproduce the experimental setup of Ref. 6.

(v) For the numerical integration of the rate equations, we have used 20 values of k between 0 and k_{obs}, and between k_{obs} and $k_{\mathrm{rad.}}$. 100 rings have been defined between k_{rad} and $k_{\mathrm{max}}=5\times10^{-2}$ Å^{-1}.

III. RESONANT EXCITATION OF THE POLARITON STATES

In this section, we first calculate decay curves of the lower-energy polariton states under resonant excitation (1.5 ps pulse). Therefore in the calculation, we create polaritons around the initial time in the lower branch with an in-plane wave vector k_{ex} and calculate the intensity of light emitted by the lower branch in the detection cone ($0\leqslant k\leqslant k_{\mathrm{obs}}$).

Figure 1(a) presents calculated decay curves for three different detuning δ and a temperature of 10 K. In agreement with experimental results,[6] we find a biexponential decay for positive detunings. By analyzing in detail the polariton transfers versus time, we confirm that the short decay corresponds either to the immediate escape of the polariton or to the absorption of phonons and the scattering towards large **k** (the reservoir). The short-time behavior is therefore well described by the simple equation (1). The second slower decay is then due to the return from the reservoir towards the radiant states under examination.

In Fig. 1(b) we plotted the calculated and measured initial decay times under resonant excitation. An excellent agreement between calculation and experiments is obtained for a large range of detuning and with no adjustable parameter.

Figure 2 shows the polariton in-plane dispersion relations and the lower branch exciton weight for two opposite detunings. For a detuning equal to $+6$ meV, the dispersion of the lower branch is similar to that of the uncoupled exciton and its exciton weight is very close to 1, even in the center of the

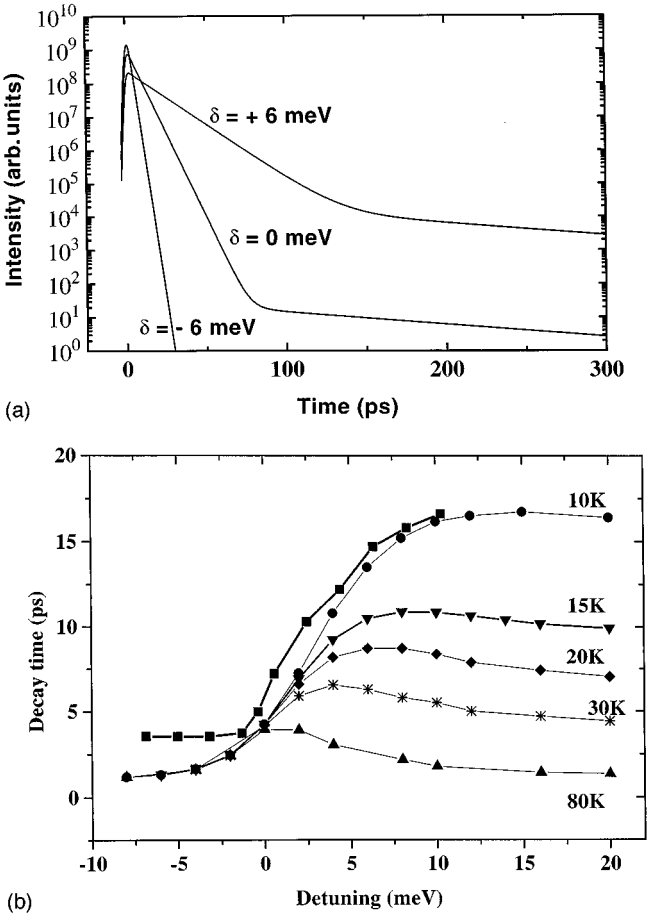

FIG. 1. (a) Calculated decay curves for three detunings $\delta = -6$, 0, and $+6$ meV. (b) (■) Experimental initial decay time (taken from Ref. 6) measured at 10 K as a function of the detuning δ. Other curves: calculated decay time for different temperatures.

Brillouin zone. Since the polariton escape time is very long in this range of detunings, the decay curves are mainly governed by acoustic-phonon scattering. In Ref. 6, we reported that similar decay curves were measured in a cavity sample for positive detunings and in a reference sample without top mirror. However, in the reference sample, the short photoluminescence (PL) decay time is not only controlled by the acoustic-phonon scattering (which is identical in the cavity sample), but also by the exciton radiative lifetime characteristic of the coupling to the continuum of photon modes (in the absence of cavity). Probably because these two terms are of the same order of magnitude (≈ 10 ps), similar behaviors are observed for positive detunings in the case of polaritons and for the bare exciton. On the contrary, for negative detunings, the curvature of the lower branch in the center of the Brillouin zone is much larger and at the same time the exciton weight of these polaritons is very small. These states are mainly photonlike and their scattering by acoustic phonon is inefficient.[13] Therefore, most of the initially created polaritons immediately emit a photon: the initial decay is very fast and the second slow decay is not visible, in agreement with experiments.[6]

Figure 1(b) also presents the calculated initial decay time versus detuning for different temperatures. When increasing the temperature, scattering by acoustic phonons becomes

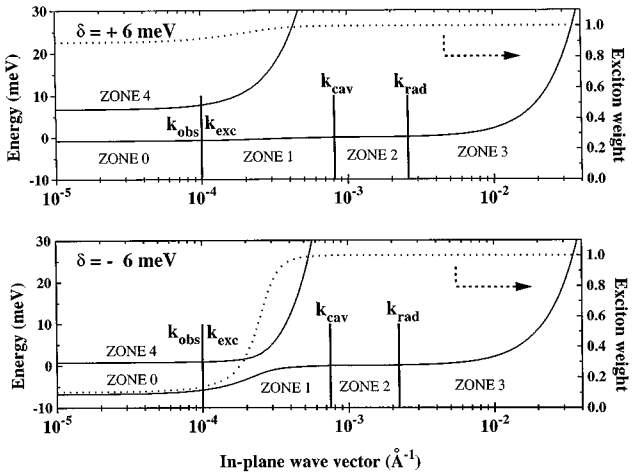

FIG. 2. In-plane dispersion relations (solid lines) of the polaritons for two opposite detunings ($\delta = +6$ and -6 meV). The dashed lines indicate the exciton weight of the lower energy polariton as a function of the in-plane wave vector. Vertical bars show the position of the characteristic wave vectors used in the calculation, namely, k_{obs}, k_{exc}, k_{cav}, and k_{rad}.

more and more efficient so that the decay time is reduced for positive detunings. Moreover, at low temperatures, the decay time increases strongly and monotonously with the detuning whereas for a temperature superior to 30 K, it presents a slight maximum near zero. To our knowledge, these evolutions with temperature have not yet been checked experimentally.

We now consider the decay curves at long-time delays in a more quantitative way. At 10 K, the relative intensity of the second decay for positive detunings is three orders of magnitude smaller in the calculation than in the experiments. However, it is of importance to recall that in these experiments, the laser reflected beam had been masked by a little screen. Therefore, for short-time delays, only light coming out from polaritons which have been elastically scattered can be detected. Since in the calculation, we count the whole emission of the ring of in-plane wave vector k_{exc}, we overestimate the first decay with respect to the long-time tale. This could explain a part of the discrepancy between experiment and calculation. To include the fact that one ring in k space is partially masked, we introduced a phenomenological parameter α which reflects the proportion of light, emitted by the ring of in-plane wave vector k_{exc}, which is counted in the total signal $I(t)$. For short-time delays, α corresponds to the fraction of polaritons elastically scattered. Except for large positive detunings, the introduction of α does not change the short or the long decay time but only modifies the relative intensity of these decays. For positive detunings, we reproduce the global experimental decay curves with $\alpha = 10^{-3}$. This may indicate that the elastic scattering rate leading to an isotropic population of the rings in k space is not as short as previously measured in bare quantum wells.[16] However, even with this value of α, the calculated relative intensity of the second decay for a detuning $\delta = 0$ is still two orders of magnitude smaller than in the experimental data (instead of five for $\alpha = 0$). Disorder effects may account for the remaining discrepancy. To further increase the calculated long-time tail, we have to introduce a broadening in k space, which

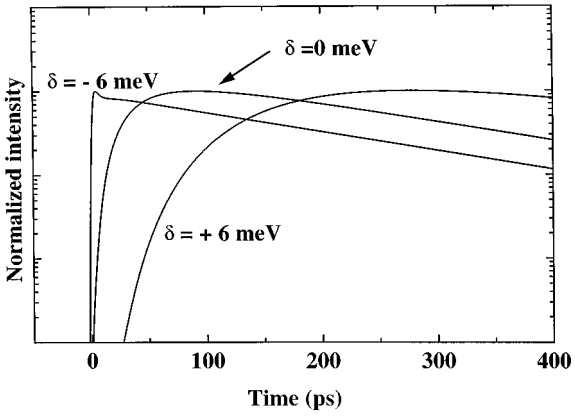

FIG. 3. Normalized calculated decay curves of the lower branch under excitation resonant to the upper branch for three detunings $\delta = -6$, 0, and $+6$ meV.

reflects disorder effects and relaxes all k related selection rules in the transition rates from Eqs. (18) and (21). This adds new phenomenological parameters and we would need additional experimental data to adjust them. Moreover, to properly take into account the polariton inhomogeneous broadening, we would have to make the full calculation of broadened excitons coupled to the cavity mode as in Ref. 17. Then the scattering by acoustic phonons between these new broadened polariton states has to be calculated. Recently, Whittaker *et al.* showed that the influence of disorder and the induced broadening strongly depends on the detuning because of the change in the polariton effective mass. When this mass is getting smaller, motional narrowing is observed.[18] Moreover, in Ref. 19 they showed that the nature of the exciton and cavity mode broadening, strongly influences the resulting polariton broadening. Therefore, a precise microscopic description of the disorder is necessary to calculate the polariton inhomogeneous broadening but is beyond the scope of the present work.

Finally, we also calculated decay curves of the upper polariton branch under resonant excitation. Similar results are found. The luminescence of the upper polariton decays biexponentially. As for the lower polariton, the first decay time gets shorter when the upper polariton becomes photonlike and at the same time, the relative intensity of the second decay becomes smaller. As is mentioned in Ref. 20, we found that for a similar exciton and photon weight, the first decay time is shorter for the upper polariton since it involves the emission of acoustic phonons, whereas for the lower polariton, absorption of acoustic phonons is required. These calculations describe qualitatively the experimental decay curves in Ref. 6 of the upper polariton branch under resonant excitation.

IV. EXCITATION RESONANT TO THE UPPER ENERGY POLARITON STATE

In this section, we calculate decay curves of the lower-energy polariton states under an excitation resonant to the upper polariton as in Ref. 11 (1.5 ps pulse). Therefore, we create polaritons around the initial time in the upper branch with the same in-plane wave vector k_{exc} as in the previous section and calculate the intensity of light emitted by the

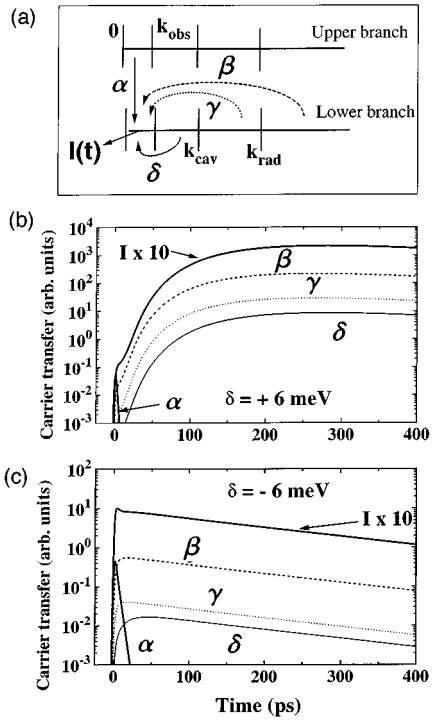

FIG. 4. (a) Schematic graph of the calculated transfers α, β, γ, and δ, from different zones of k space toward the detection cone. (b) and (c) Calculated transfers as a function of time from different zones of k space toward the detection cone. The signal intensity $I(t)$, which is roughly proportional to the sum of these transfers, is also shown. (b) Corresponds to $\delta = +6$ meV whereas (c) corresponds to $\delta = -6$ meV.

lower branch in the detection cone ($0 \leqslant k \leqslant k_{obs}$). Figure 3 presents lower branch decay curves for two opposite detunings. Both rise time and decay time are shortened when moving from positive to negative detunings, in qualitative agreement with experimental curves presented in Ref. 11.

In order to get a better understanding of the destiny of the polaritons initially created in the upper branch, we define five regions in k space, as shown in Fig. 2, and look at the transfers between these zones as a function of time. The four first zones concern the lower branch: Zone 0 corresponds to the detection cone ($0 \leqslant k \leqslant k_{obs}$), zone 1 to radiant states in the strong coupling regime but out of the detection cone ($k_{obs} \leqslant k \leqslant k_{cav}$), zone 2 to radiant states in weak coupling ($k_{cav} \leqslant k \leqslant k_{rad}$), and zone 3 to nonradiant states ($k_{rad} \leqslant k$). Finally, zone 4 describes the detection cone in the upper branch ($0 \leqslant k \leqslant k_{obs}$) where carriers are initially injected in our calculation. Figure 4 shows the number of carriers transferred from one of these zones to zone 0 as a function of time and for the two considered detunings $+6$ and -6 meV. For a positive detuning, almost all carriers are initially transferred to zone 3, the reservoir of nonradiant states. Then a fraction of them are transferred to zone 0, and the shape of the whole luminescence curve essentially reflects this transfer from zone 3 to zone 0. However, for a negative detuning, since the polariton states of zone 0 are mainly photonlike, scatterings to this zone are inefficient. Most of the carriers are initially scattered through zone 3 as in the previous case but then they mainly recombine through oblique modes in zones 1 and 2. Very few carriers are scattered to zone 0 and

this transfer is of the same order of magnitude than the direct transfer from zone 4 to zone 0. Therefore, the short rise time reflects this direct transfer from the upper branch to the detection cone and the decay time corresponds to the emptying of zone 3. In both cases the decay time of the luminescence is governed by the evolution of the nonradiant state population and therefore is weakly sensitive to cavity effects.

The calculated intensity of light strongly decreases when the lower branch becomes photonlike. However, the opposite behavior is observed experimentally: a much more intense signal is detected for a photonlike lower branch (negative detuning). This discrepancy clearly indicates that our model of perfect delocalized polaritons, which does not take into account any disorder, only gives a qualitative description of nonresonant luminescence.

V. CONCLUSION

Under resonant excitation, the PL decay time is significantly shortened when the lower-energy state is photonlike. However, we would like to underline here that this is the case only because we excite the system resonantly to the states that are in the strong-coupling regime. Actually these states with $0 \leqslant k \leqslant k_{cav}$ represent only a small fraction of the radiant states (roughly 10%). 90% of the radiant states are weakly coupled to photons and their spontaneous emission is only slightly modified by cavity effect (through the modification of oblique modes). Therefore, the overall spontaneous emission rate is unchanged: this is consistent with Ref. 4 where Stanley *et al.* showed that the integrated intensity of light emitted by the edge of a microcavity does not depend on the detuning. They conclude that cavity effects only concern a very small proportion of the radiant states.

When carriers are created at higher energy than the ground state, essentially states weakly coupled to the cavity mode are populated at initial times and they mainly emit light through the leaky modes of the Bragg mirrors. As in Ref. 14, we also calculated the decay time of a sharply peaked excitonic population at the energy of the exciton continuum and found, in agreement with Tassone *et al.*, weak dependance of the overall dynamics on the detuning between cavity and exciton. In the present calculation however, since we create the initial carrier population resonantly on the upper branch, we find a strong dependence of the rise time on the detuning in agreement with experiments. But as in Ref. 14, after a few picoseconds, the carriers thermally fill the reservoir and then the luminescence decay reflects the emptying of the reservoir and therefore weakly changes with detuning.

In conclusion, our model describes very well the short-time behavior of resonant luminescence measured in samples described in Ref. 6. It also gives a qualitative understanding of the overall dynamics over a larger time scale. However, to describe precisely the experimental long-time behavior of the bare quantum-well exciton, we have to introduce a very large broadening in k space. With such a broadening of the polariton states, the border between the strong- and the weak-coupling zone is blurred. Therefore, in such samples, disorder cannot be treated as a small perturbation of perfectly delocalized polaritons. It would thus be very interesting to compare our calculated decay curves with time-resolved measurements in microcavities where a Rabi splitting much larger than the PL line broadening was reported, such as II-VI microcavities.[5]

ACKNOWLEDGMENTS

We would like to acknowledge B. Sermage, R. Planel, and I. Abram for fruitful discussions.

*Electronic address: jacqueline.bloch@bagneux.cnet.fr

[1] C. Weisbuch, M. Nishioka, A. Ishikawa, and Y. Arakawa, Phys. Rev. Lett. **69**, 3314 (1992).

[2] R. Houdré, C. Weisbuch, R. P. Stanley, U. Oesterle, P. Pellandini, and M. Ilegems, Phys. Rev. Lett. **73**, 2043 (1994).

[3] T. A. Fisher, A. M. Afshar, D. M. Whittaker, and M. Skolnick, Phys. Rev. B **51**, 2600 (1995).

[4] R. P. Stanley, R. Houdré, C. Weisbuch, U. Oesterle, and M. Ilegems, Phys. Rev. B **53**, 10 995 (1996).

[5] P. Kelkar, V. Kozlov, H. Jeon, A. V. Nurmikko, C.-C. Chu, D. C. Grillo, J. Han, C. G. Hua, and R. L. Gunshor, Phys. Rev. B **52**, R5491 (1995).

[6] B. Sermage, S. Long, I. Abram, J. Y. Marzin, J. Bloch, R. Planel, and V. Thierry-Mieg, Phys. Rev. B **53**, 16 516 (1996).

[7] T. B. Norris, J. K. Rhee, C. Y. Sung, Y. Arakawa, M. Nishioka, and C. Weisbuch, Phys. Rev. B **50**, 14 663 (1994).

[8] K. Tanaka, T. Nakamura, W. Takamatsu, M. Yamanishi, Y. Lee, and T. Ishihara, Phys. Rev. Lett. **74**, 3380 (1995).

[9] J. Jacobson, S. Pau, H. Cao, G. Björk, and Y. Yamamoto, Phys. Rev. A **51**, 2542 (1995).

[10] J. Wainstain, G. Cassabois, Ph. Roussignol, C. Delalande, M. Voos, F. Tassone, R. Houdré, R. P. Stanley, and U. Oesterle (unpublished).

[11] J. Bloch, V. Thierry-Mieg, R. Planel, B. Sermage, S. Long, and I. Abram, Solid-State Electron. **40**, 487 (1996).

[12] B. Deveaud, F. Clerot, N. Toy, K. Satzke, B. Sermage, and D. S. Katzer, Phys. Rev. Lett. **67**, 2355 (1991).

[13] S. Pau, G. Björk, J. Jacobson, H. Cao, and Y. Yamamoto, Phys. Rev. B **51**, 7090 (1995).

[14] F. Tassone, C. Piermarocchi, V. Savona, and A. Quattropani, Phys. Rev. B **53**, R7642 (1996).

[15] U. Bockelmann, Phys. Rev. B **48**, 17 637 (1993).

[16] Hailing Wang, Jagdeep Shah, T. C. Damen, and L. N. Pfeiffer, Phys. Rev. Lett. **74**, 3065 (1995).

[17] V. Savona and C. Weisbuch, Phys. Rev. B **54**, 10 835 (1996).

[18] D. M. Whittaker, P. Kinsler, T. A. Fisher, M. S. Skolnick, A. Armitage, A. M. Afshar, M. D. Sturge, and J. S. Roberts, Phys. Rev. Lett. **77**, 4792 (1996).

[19] P. Kinsler and D. M. Whittaker, Phys. Rev. B **54**, 4988 (1996).

[20] F. Tassone, C. Piermarocchi, V. Savona, A. Quattropani, and P. Schwendimann, in ''*Microcavities and Photonic Bandgaps: Physics and Applications*,'' Vol. 324 of *NATO Advanced Studies Institute, Series E*, edited by J. Rarity and C. Weisbuch (Kluwer Academic, Dordrecht, 1996).